

UCSF

UC San Francisco Previously Published Works

Title

Quantitative brain MRI morphology in severe and attenuated forms of mucopolysaccharidosis type I

Permalink

<https://escholarship.org/uc/item/4141853f>

Journal

Molecular Genetics and Metabolism, 135(2)

ISSN

1096-7192

Authors

Kovac, Victor
Shapiro, Elsa G
Rudser, Kyle D
[et al.](#)

Publication Date

2022-02-01

DOI

10.1016/j.ymgme.2022.01.001

Peer reviewed



HHS Public Access

Author manuscript

Mol Genet Metab. Author manuscript; available in PMC 2023 February 01.

Published in final edited form as:

Mol Genet Metab. 2022 February ; 135(2): 122–132. doi:10.1016/j.ymgme.2022.01.001.

*Corresponding author at: Department of Pediatrics, Masonic Institute for the Developing Brain (MIDB), University of Minnesota, 2025 E River Pkwy, Minneapolis, MN 55414, USA. nestr007@umn.edu (I. Nestrasil).

¹Currently at the Brigham and Women’s Hospital, Harvard Medical School, Boston, MA, USA.

²Currently at BioMarin Pharmaceutical, San Rafael, CA.

³Currently at the Department of Inherited Metabolic Diseases, Birmingham Children’s Hospital, UK.

⁴Currently at the Departments of Pediatrics & Ophthalmology, University of California Davis, Sacramento, CA, USA.

⁵Currently at the Department of Laboratory Medicine and Pathology, Mayo Clinic, Rochester, MN, USA.

Author Contributions

Name	Location	Contribution
Victor Kovac	University of Minnesota, Minneapolis	Drafted and revised the manuscript for intellectual content. Major role in MRI data collection and analysis.
Elsa G. Shapiro	University of Minnesota, Minneapolis	Designed the study, directed research, guided the neuropsychological data interpretation, assisted in writing the manuscript with extensive revising and editing for intellectual content.
Kyle D. Rudser	University of Minnesota, Minneapolis	Provided statistical analysis, including writing/editing of that section. Generated graphics. Revised and edited draft for intellectual content.
Bryon A. Mueller	University of Minnesota, Minneapolis	Designed the MRI imaging protocol and guided the MRI data acquisition. Revised and edited draft for intellectual content.
Julie B. Eisengart	University of Minnesota, Minneapolis	Major role in neuropsychological data collection, analysis and interpretation. Provided extensive revising and editing for intellectual content.
Kathleen A. Delaney	University of Minnesota, Minneapolis	Major role in neuropsychological data collection. Revised and edited draft for intellectual content.
Alia Ahmed	University of Minnesota, Minneapolis	Assisted in MRI data analysis. Revised and edited draft for intellectual content.
Kelly E. King	University of Minnesota, Minneapolis	Provided neuropsychological data interpretation. Revised and edited draft for intellectual content.
Brianna D. Yund	University of Minnesota, Minneapolis	Provided neuropsychological data collection and analysis of 4-7-year old controls. Revised and edited draft for intellectual content.
Morton J. Cowan	University of California, San Francisco	Revised and edited draft for intellectual content. Leadership and data collection at the site.
Julian Raiman	University of Toronto, Toronto, Canada	Revised and edited draft for intellectual content. Leadership and data collection at the site.
Eva G. Mamak	Hospital for Sick Children, Canada	Revised and edited draft for intellectual content. Leadership and data collection at the site.
Paul R. Harmatz	University of California, San Francisco	Revised and edited draft for intellectual content. Leadership and data collection at the site.
Suma Shankar	Emory University, Atlanta	Revised and edited draft for intellectual content. Leadership and data collection at the site.
Nadia Ali	Emory University, Atlanta	Revised and edited draft for intellectual content. Leadership and data collection at the site.
Stephanie Cagle	Emory University, Atlanta	Revised and edited draft for intellectual content. Leadership and data collection at the site.
Jeffrey R. Wozniak	University of Minnesota, Minneapolis	Collected, analyzed control MRI data for participants over 8 years old. Revised and edited draft for intellectual content.
Kelvin O. Lim	University of Minnesota, Minneapolis	Collected, analyzed control MRI data for participants over 8 years old.

Author Manuscript

Author Manuscript

Author Manuscript

Author Manuscript

Quantitative brain MRI morphology in severe and attenuated forms of mucopolysaccharidosis type I

Victor Kovac^{a,1}, Elsa G. Shapiro^a, Kyle D. Rudser^b, Bryon A. Mueller^c, Julie B. Eisengart^a, Kathleen A. Delaney^{a,2}, Alia Ahmed^a, Kelly E. King^a, Brianna D. Yund^a, Morton J. Cowan^d, Julian Raiman^{e,3}, Eva G. Mamak^f, Paul R. Harmatz^g, Suma P. Shankar^{h,4}, Nadia Aliⁱ, Stephanie R. Cagle^{i,5}, Jeffrey R. Wozniak^c, Kelvin O. Lim^c, Paul J. Orchard^j, Chester B. Whitley^k, Igor Nestrasil^{l,*}

^aDivision of Clinical Behavioral Neuroscience, Department of Pediatrics, University of Minnesota, Minneapolis, MN, USA

^bDivision of Biostatistics, School of Public Health, University of Minnesota, Minneapolis, MN, USA

^cDepartment of Psychiatry & Behavioral Sciences, University of Minnesota, Minneapolis, MN, USA

^dUCSF Benioff Children's Hospital, University of California, San Francisco, CA, USA

^eDivision of Clinical and Metabolic Genetics, Department of Paediatrics, University of Toronto, The Hospital for Sick Children, Toronto, ON, Canada

^fDepartment of Psychology, The Hospital for Sick Children, Toronto, ON, Canada

^gUCSF Benioff Children's Hospital Oakland, Oakland, CA, USA

^hDepartment of Ophthalmology and Human Genetics, Emory University, Atlanta, GA, USA

ⁱDepartment of Human Genetics, Emory University, Atlanta, GA, USA

^jDivision of Pediatric Blood & Marrow Transplantation, Department of Pediatrics, University of Minnesota, Minneapolis, MN, USA

^kGene Therapy Center, Department of Pediatrics, University of Minnesota, Minneapolis, MN, USA

Name	Location	Contribution
		Revised and edited draft for intellectual content.
Paul J. Orchard	University of Minnesota, Minneapolis	Leadership on data collection of the MPS I participants scanned at the hospital (UMN site). Revised and edited draft for intellectual content.
Chester B. Whitley	University of Minnesota, Minneapolis	Provided scientific expertise in genetics. Revised and edited draft for intellectual content.
Igor Nestrasil	University of Minnesota, Minneapolis	Drafted and revised the manuscript for intellectual content. Leadership role on the scientific aspects of neuroimaging.

Publisher's Disclaimer: This is a PDF file of an unedited manuscript that has been accepted for publication. As a service to our customers we are providing this early version of the manuscript. The manuscript will undergo copyediting, typesetting, and review of the resulting proof before it is published in its final form. Please note that during the production process errors may be discovered which could affect the content, and all legal disclaimers that apply to the journal pertain.

¹Division of Clinical Behavioral Neuroscience, Department of Pediatrics, University of Minnesota, Center for Magnetic Resonance Research (CMRR), Department of Radiology, Minneapolis, MN, USA

Abstract

Objective: To assess our hypothesis that brain macrostructure is different in individuals with mucopolysaccharidosis type I (MPS I) and healthy controls (HC), we conducted a comprehensive multicenter study using a uniform quantitative magnetic resonance imaging (qMRI) protocol, with analyses that account for the effects of disease phenotype, age, and cognition.

Methods: Brain MRIs in 23 individuals with attenuated (MPS IA) and 38 with severe MPS I (MPS IH), aged 4-25 years, enrolled under the study protocol [NCT01870375](#), were compared to 98 healthy controls.

Results: Cortical and subcortical gray matter, white matter, corpus callosum, ventricular and choroid plexus volumes in MPS I significantly differed from HC. Thicker cortex, lower white matter and corpus callosum volumes were already present at the youngest MPS I participants aged 4-5 years. Age-related differences were observed in both MPS I groups, but most markedly in MPS IH, particularly in cortical gray matter metrics. IQ scores were inversely associated with ventricular volume in both MPS I groups and were positively associated with cortical thickness only in MPS IA.

Conclusions: Quantitatively-derived MRI measures distinguished MPS I participants from HC as well as severe from attenuated forms. Age-related neurodevelopmental trajectories in both MPS I forms differed from HC. The extent to which brain structure is altered by disease, potentially spared by treatment, and how it relates to neurocognitive dysfunction needs further exploration.

Keywords

mucopolysaccharidosis; Hurler Scheie syndrome; brain MRI; quantitative brain volumetry; ventricle; cortex

1. Introduction

Novel treatments for mucopolysaccharidosis type I (MPS I) aim to minimize the central nervous system (CNS) morbidity making the precise quantification of brain abnormalities critical for the characterization of the anticipated disease course and detection of potential treatment effects. To accomplish this, a uniform quantitative magnetic resonance imaging (qMRI) volumetric protocol was established to assess developmental (age-related) changes in severe and attenuated forms of MPS I.

Cerebral white matter (WM) abnormalities, ventricular enlargement, brain atrophy, and enlarged perivascular spaces are prevalent findings in the MPS I brain and can be rated by severity scales¹⁻³. Most studies have relied on qualitative radiological evaluations, as opposed to fully quantitative techniques that provide reproducible and precise measurements of neuroanatomy⁴. The application of automated techniques is exceptionally challenging

and often requires meticulous correction during post-processing analysis due to prominent morphologic abnormalities seen in the brains of patients with MPS I⁴.

Previous work employing qMRI automated brain volumetry has implicated WM and gray matter (GM) alterations and their association with IQ and attention in treated MPS I patients⁵⁻⁸.

This study applied automated volumetric analysis to the brains of individuals with MPS I and compared absolute and age-related differences between severe and attenuated phenotypes and healthy controls (HC). We hypothesized that lower WM and corpus callosum (CC) volumes are present in MPS I and that cortical and subcortical GM volumes in MPS I are lower than in HC. Finally, we postulated that intelligence is positively associated with cortical GM-derived metrics, WM, and thalamic volumes but negatively with ventricular volume, consistent with healthy pediatric population studies⁹⁻¹².

2. Material and methods

2.1. Subjects

One hundred fifteen study participants with MPS I were enrolled in the longitudinal protocol [NCT01870375](#) of the Lysosomal Disease Network (Longitudinal Studies of Brain Structure and Function) with the following inclusion criteria: confirmed diagnosis of MPS I, physically able to undergo a 1-hour non-sedated scan, and hearing and vision adequate for neuropsychological testing. Of the 115 MPS I participants, 98 had scans following the MRI study protocol. Eligible participants were between 4 and 24 years of age and had no ventricular shunt. Participants with ventricular shunts were not included because of the effect of shunts on brain and ventricular volumes. No participants below four years of age were included in this study due to the challenges of scanning without sedation and limited GM/WM contrast in this age group, which can preclude precise automated brain segmentation. Sixty-one of the 98 MPS I participants met inclusion criteria for this report. Thirteen participants were included even though they had a scan under sedation. Thirty-eight participants with the severe form of MPS I, Hurler syndrome (MPS IH), and 23 participants with one of the attenuated forms of MPS I, Hurler-Scheie and Scheie syndromes (MPS IA) were included. The measurements of the HC group were collected from three separate studies using the same inclusion criteria and consisted of 98 participants.

Although participants were seen yearly, the data presented here are cross-sectional, as longitudinal data from HC were not available for comparison. Therefore, age-matched MPS IH, MPS IA, and HC groups were created by selecting the earliest analyzable scan from the longitudinal datasets. Participants with MPS IH were 9.5-22.8 (median 8.5) years post-hematopoietic stem cell transplantation (HSCT), and all participants with MPS IA had been on enzyme replacement therapy (ERT) for 0.5-12.5 (median 6.9) years prior to scan acquisition (Table 1). Four MPS IH participants received intrathecal ERT prior to the HSCT.

2.2. Standard Protocol Approvals, Registrations, and Patient Consents

Study participants were scanned at five centers (Table 1). All centers had IRB approval for this study, and all participants, parents, and/or legal guardians gave signed informed consent;

assent was obtained from children and those over 18 years with legal guardians at their home institution, which included permission to share de-identified data with the RDCRN (Rare Disease Clinical Research Network) Data Monitoring and Coordination Center and with the University of Minnesota for data analysis.

2.3. Neuropsychological evaluation

As previous studies have used IQ tests as a functional outcome measure in relationship to MRI data, we included the Full Scale IQ. One of two IQ tests was administered to MPS participants as previously described⁵: The Wechsler Preschool and Primary Scale of Intelligence, Third Edition, for participants from 4 to 6 years of age and the Wechsler Abbreviated Scale of Intelligence for participants over six years. All assessments, which were concurrent with the MRI exam dates, were administered by trained personnel who had extensive experience with MPS participants and these tests. Healthy controls were administered these same tests, except in the case of the 4-8-year-old HC who were administered the Kaufman Brief Intelligence Test, Second Edition, allowing for comparison of IQ scores between groups.

2.4. MRI

2.4.1. Data acquisition—Fifty-seven MPS participants were examined with 3-T Siemens scanners (Siemens, AG, Erlangen, Germany) with 12-channel (Siemens Trio)/20-channel (Siemens Skyra) RF head coils. The MRI protocol included an 11-minute 3-dimensional, T1-weighted, magnetization-prepared rapid acquisition with gradient-echo (MPRAGE) sequence (TR/TE/TI: 2530/3.65/1100 ms; voxel size: $1 \times 1 \times 1 \text{ mm}^3$; 240 slices; no gap; bandwidth: 180 Hz/pix; field-of-view (FoV): 256 mm). Four participants (at the San Francisco site) were scanned on a 3-T Phillips Achieva scanner (Philips Medical Systems, Best, the Netherlands) with a SENSE-NV-16-channel head coil that included a 10-min 3-dimensional, T1-weighted turbo field echo TFE sequence (TR/TE: 8270/3.79 ms; voxel size $1 \times 1 \times 1 \text{ mm}^3$; no gap; FOV: $256 \times 256 \times 176 \text{ mm}$; bandwidth: 191 Hz/pix). The Philips TFE protocol was equivalent to Siemens MPRAGE protocol. The study site underwent the quality control including the phantom and healthy subject scans prior to the site activation.

During imaging, most participants watched a movie in a research-dedicated scanner to improve cooperation and reduce movement. For young participants who required sedation (n=13), clinical scans using the same parameters were used with the local IRB permission.

All controls were examined with the research-dedicated 3-T Trio scanner using a 5-minute MPRAGE sequence with the same parameters, but a GRAPPA factor of 2 was utilized.

2.4.2. Image analysis—Volumetric analysis was conducted using FreeSurfer (FS) Image Analysis Suite¹³, version 5.3, which yields surface-based cortical parcellation and volume-based morphometric segmentation. In this analysis, the volumes of cortical cerebral and cerebellar GM and WM, CC, choroid plexus (ChP), thalamus, hippocampus, amygdala, putamen, pallidum, and caudate were assessed. Additionally, total ventricular volume, intracranial volume (ICV), mean cortical surface area (CSA), and cortical thickness (CTh)

were determined. Left and right volumes of bilateral structures were summed and reported as one total volume. All segmentations were visually inspected and manually corrected if necessary (Section 2.3.3).

2.4.3. Manual adjustments—Manual editing was required in 43% of MPS I scans. Abnormal brain morphology, particularly enlarged ventricles, enlarged perivascular spaces, and thickened dura, were the most common causes of aberrant automated volumetric analysis. Manually selected “control points” were placed on high-intensity voxels that were identified as white matter but omitted in the initial automated segmentation. Control points re-threshold the intensity of selected and neighboring voxels to the threshold intensity of white matter (Fig. 1A). The new iteration was run with the *-autorecon2-cp* flag. In four cases with severely enlarged lateral ventricles, the CSF regions corresponding to the lateral ventricles were left un-segmented by initial processing and had to be either re-run with *-bigventricles* flag or manually “filled” using the Freesurfer tkmedit tool and re-run with *-autorecon2-wm* flag (Fig. 1B)¹⁴. After re-analyzing the edited scans, all were re-inspected for accuracy. In cases of inaccuracy, subsequent rounds of edits and FS analysis were performed. Analysis typically required one to four iterations of edits to obtain satisfactory results.

2.5. Statistical analysis

Descriptive statistics were tabulated separately for MPS IH, MPS IA, and HC groups. These included the mean and standard deviation for continuous variables and frequency with percentage for categorical variables. All MRI variables were reported unadjusted and adjusted for the ICV (i.e., as a fraction of ICV). Differences in means were evaluated using the t-test with unequal variance and Welch degrees of freedom. First order linear trends of volumes across chronological age are based on least squares regression estimates with robust variance estimation for confidence intervals and P-values. Differences in slopes were evaluated by testing interaction terms in regression models. All analyses were conducted using R v2.15.2¹⁵.

2.6. Data Availability Statement

All data has been uploaded into the Data Management and Coordinating Center (DMCC) for the Rare Diseases Clinical Research Network (RDCRN). The DMCC is a secure clinical data management system to collect and store data on a variety of rare diseases from organizations across the United States. The data are held in the DMCC for five years after which they are released to the database of Genotypes and Phenotypes (dbGaP).

3. Results

3.1. Demographic information and IQ

The Full Scale IQ scores were below the population mean (1.3 standard deviations) in MPS IH; in the MPS IA group, the IQ was almost 0.5 standard deviation below the population mean (Table 1).

3.2. Brain MRI measure differences and comparison of MPS I groups to healthy controls

Mean CSA and volumes of cerebral WM, CC, thalamus, and pallidum were lower in MPS IH < MPS IA < HC (Table 2, Figure 2). Cortical thickness was higher in MPS IH > MPS IA > HC. Total ventricular and ChP volumes were higher in both MPS groups (slightly MPS IA > MPS IH) than HC. Intracranial volumes were not significantly different between all groups. Hippocampus volume was lower in the MPS IA group. Post-hoc Pearson correlation analysis showed significant correlations between ventricular and ChP volumes in all groups with $R = 0.74/0.68/0.54$ for MPS IH/MPS IA /HC, respectively (all $p < 0.001$).

3.3. Age-related differences in brain MRI measures with the comparison of linear trends between MPS I groups and healthy controls

Volumes of cerebral WM and cortical GM unadjusted for ICV in MPS IH and ChP in both MPS groups (MPS IA > MPS IH) showed significant associations with age (Table 3A, Figure 2). For ICV-adjusted volumes, CC and putamen in MPS IH, pallidum in MPS IA, cortical GM in both MPS groups (MPS IA < MPS IH), and ChP in both MPS groups (MPS IA > MPS IH) were associated with age. In addition, CTh was lower with age in all groups (MPS IH > MPS IA > HC).

The comparison of age-related slopes for brain MRI metrics between groups is summarized in Table 3B. Between MPS IH and MPS IA participants, there were no significant differences in slopes. However, for ICV-unadjusted measures, the slopes differed between MPS IH and HC in the CC, amygdala, thalamus, ChP, CSA, CTh, and cortical GM; the slopes between MPS IA and HC differed in the amygdala, ChP, pallidum, and thalamus. For ICV-adjusted volumes, the slopes differed between MPS IH and HC in the CC, amygdala, thalamus, ChP, and cortical GM; the slopes between MPS IA and HC differed in the ChP and thalamus.

3.4. Association of brain MRI measures and IQ with the comparison of linear trends between MPS I groups and healthy controls

High IQ values were associated with high ICV-unadjusted cortical GM volumes, low ICV-unadjusted and ICV-adjusted ventricular volumes, and high CTh only in the MPS IA group. Comparison of IQ scores vs. CTh revealed the positive relationship for MPS IA and the negative relationship for both HC and MPS IH. In addition, the comparison of IQ scores vs. ventricular volume differed between MPS IA and HC and between MPS IH and HC (Table 4, Figure 3).

4. Discussion

This study systematically measured MPS I-related changes in brain macrostructure with quantitative MRI to investigate potential differences between phenotypes and compare the magnitude of abnormality to healthy controls. Cortical gray and white matter, CC, thalamus and globus pallidum, ventricles and ChP were altered in this cross-sectional study of participants with attenuated and severe forms of MPS I. Cortical GM-derived measures, including cortical thickness, CC, thalamus, and ChP volumes showed age-related differences in both MPS I groups but were most pronounced in MPS IH. Significant IQ-related

associations were present for ventricular volume in both MPS I forms and cortical thickness in MPS IA. The findings of this study suggest that distinct differences exist between severe and attenuated forms of MPS I as assessed by quantitative MRI.

MPS I is a rare autosomal recessive disease caused by mutations in the alpha-L-iduronidase (*IDUA*) coding gene. These mutations lead to the absence or insufficient levels of the lysosomal *IDUA* hydrolytic enzyme responsible for the breakdown of large sugar molecules called glycosaminoglycans (GAG)^{16, 17}. As a result, GAG accumulate in various organ systems, including the CNS, leading to multisystem dysfunction and neurological disease of varying severity^{5, 17}. The severe form of the disease, Hurler syndrome (MPS IH), is treated by hematopoietic stem cell transplantation (HSCT) to halt neurological and cognitive deterioration and prevent death. Individuals with the same enzymatic deficiency, but the later onset of clinical symptoms, are diagnosed with Scheie (mild) and Hurler-Scheie (intermediate) syndromes. As no biochemical differences have been found and clinical manifestations in Scheie and Hurler-Scheie syndromes overlap, both are referred to collectively as MPS I attenuated (MPS IA)^{5, 18}. Intravenous recombinant enzyme replacement therapy (ERT) is the standard of care for patients with MPS IA, as it improves somatic aspects of the disease¹⁹. However, the intravenous enzyme does not cross the blood-brain barrier (BBB) at recommended doses and has no direct therapeutic effect on brain disease^{20, 21}.

4.1. Automated brain segmentation in MPS I

Quantitative MRI studies evaluating brain abnormality by fully automated processing pipelines in MPS I are lacking. This may be due to challenges in the analysis since abnormal brain morphology complicates the registration of brain MRIs acquired from participants with MPS to common atlas space. The automated segmentation process of scans with abnormalities such as ventriculomegaly, enlarged perivascular spaces, or extensive white matter abnormality is prone to frequent mis-segmentations of brain regions⁴. Almost half of the scans in our study required at least one manual correction of automated segmentation to yield satisfactory results. Labor-intensive manual corrections performed by an operator with expertise in neuroanatomy and subsequent re-analysis are necessary. Both add to the overall time per analysis, which needs to be considered when conducting studies with populations having similar structural brain abnormalities. Meningeal thickening due to GAG storage present in MPS I may affect the estimation of ICV by automated approaches. Intracranial volume, which is usually used to adjust brain structure size to individual head size, may be inaccurate if applied to the MPS I population. Here, both adjusted and unadjusted outcomes were applied and reported to provide a full description of the brain volumetrics.

4.2. White matter

Previous research has demonstrated reduced volumes of cerebral WM and of the major cerebral WM tract, the corpus callosum, in humans^{5, 6} and dogs²² with MPS I. Abnormal myelination as an underlying process of WM disease in MPS I has been suggested by diffusion MRI (dMRI) and neuro-histochemical animal studies²³⁻²⁵. A case study of a deceased Hurler patient reported gliosis with disruption of the normal lamellar myelination pattern leading to the destruction of the myelin sheath and axonal degeneration²⁶.

Dystrophic axons with thin myelin sheaths were found in the MPS I mouse brain²⁷. Lower WM integrity in dMRI and CC volume were shown in MPS I participants^{28, 29} and were related to attention in MPS I⁶ and MPS II attenuated participants³⁰. Our findings with a larger MPS I cohort demonstrate reduced cerebral WM and CC volumes and highlight the presence of WM abnormalities in the entire spectrum of MPS I. Maturation of WM via increases in myelin content, reflected by incremental increases in volume, is well known in neurodevelopment³¹ and also illustrated by our volumetric findings in healthy controls. White matter volumes in both MPS I groups showed an association with age that was different from the healthy controls, and was already present in the youngest MPS I participants; this was especially evident in the MPS IH group where CC volume had a negative association with age. There was a positive association between IQ and cerebral WM in HC, but, notably, no significant association existed in either MPS I group, presumably due to excess GAG accumulation in WM in participants with MPS I. GAG and other storage material affect neurons, glial cells and may result in gliosis or cell death³². Furthermore, the perivascular GAG deposition, which manifests as enlarged perivascular spaces and may be associated with glymphatic system impairment, inflammation, watershed ischemia in the deep white matter may contribute to the white matter abnormality and impaired myelination in MPS I. Absolute and age-related cerebellar WM volumes were comparable between all groups. White matter abnormalities are an important aspect of neurologic disease in both MPS IH and MPS IA. Still, longitudinal data are needed to elucidate the individual trajectories of WM development and determine the extent of the divergence from the development seen in healthy controls.

4.3. Cortical gray matter

Cortical atrophy in MPS I, as assessed by a rating scale, was observed in dogs²² and humans^{33, 34} with MPS I but was not detected in a pilot study of five MPS I and five healthy dogs when evaluated by automatically generated CTh³⁵. In the current study, cortical atrophy was measured by qMRI. Age-related slopes of cortical GM volume, CTh, and CSA deviated in both MPS I groups from HC, but only achieved statistical significance in all three measures in the MPS IH group. Linear trends showed that younger participants (even the youngest 4-5-year-old MPS I participants) had comparable cortical GM volumes and CSA but that CTh was greater in MPS IH > MPS IA > HC. Age-related expansion of CSA seen in the HC group was not observed in either MPS I group. IQ was positively associated with CTh in MPS IA participants; in contrast, IQ was negatively associated with CTh in MPS IH and HC. The observed age-related decrease in cortical GM volume in MPS I may result from equivalent cortical thinning without a commensurate expansion of CSA. The expansion of CSA is contingent upon the size of intracortical elements (neuropil) or cortical WM adjacent to specific gyrus or sulcus^{11, 36, 37} and the lack of CSA expansion in MPS I may be explained by structural alterations affecting these regions.

Histological evidence of GAG reduction has been measured after a high dose of ERT in MPS I mouse³⁸ and after intrathecal ERT administration in dog³⁹. In MPS IH, the age-related lower CTh and cortical GM volume may be explained by GAG elimination after HSCT and subsequent cortical GM reorganization, observed in normal neurodevelopment. In our dataset, age-related slopes of cortical GM-derived parameters

in MPS IA were comparable to MPS IH, except in CTh, which remained greater across ages. Glycosaminoglycan clearance from the CNS is not expected and may not explain the observed positive association of IQ and CTh, because intravenous ERT, as used for MPS IA, does not treat brain disease. It is important to note that an ongoing neurodegenerative process may also be considered given the similar slopes in both MPS I groups.

Cortical brain plasticity, measured as the size and surface area of cortical GM in MRI, is associated with human intellectual ability¹¹. Cortical GM volume over the typical lifespan follows an inverted U-shaped developmental trajectory with age⁴⁰ with its maximal peak around 10 years of age¹¹. Mean cortical thickness decreases rapidly around this same age and is stable, whereas cortical surface area expands until 12-13 years of age and afterward is stable or decreases^{11, 37}. The relationship of cortical GM metrics to IQ is complex and non-linear across the lifespan and does not simply follow the rule “more is better.” Higher IQ is associated with cortical thinning in childhood and adolescence, but this relationship is inverted in adulthood. Larger CSA is associated with higher IQ at around age 10 years, but then CSA decreases, which occurs at a higher rate in individuals with higher IQ¹¹. The age of CSA peak expansion was also shown to relate to IQ¹¹. The physiological mechanisms underlying changes in cortical microarchitecture are related to cellular and molecular events during neurodevelopment: The number of neurons and their mini-columnar organization with glial and capillary support, dendritic arborization, and ongoing GM myelination (“white matter encroachment”) contribute to cortical GM volume, CTh, and CSA^{11, 37}. Dynamic reorganization of synaptic circuitry, caused by synaptic pruning, gliogenesis, and changes in capillary support during brain maturation, may be measured by MRI as changes in cortical GM volume or thickness. Myelination in deep intracortical layers (gray/white matter boundary) during development represents a potential technical limitation in MRI evaluation of cortical GM parameters³⁷. The myelination process can result in T1-weighted signal intensity shift (signal increase) of voxels classified as GM to voxels classified as WM, which may represent a major contributor to cortical thinning measured from T1-weighted MRI in late childhood and adolescence^{37, 41}. For qMRI studies evaluating cortical GM, scans must be acquired with identical MRI sequence parameters to avoid unwanted GM/WM volumetric bias arising from differences in voxel intensity that can occur from technical discrepancies. Another critical aspect of qMRI studies of MPS participants that should not be neglected is the comparison to normal development (i.e., MRI scans of healthy controls acquired with identical imaging protocol)⁴.

4.4. Subcortical gray matter

Subcortical GM volumes also follow an inverted U-shaped developmental trajectory, similar to cortical GM,⁴⁰ that peaks around age 13-17 years⁴². Both the thalamus and globus pallidum in both MPS I groups and the hippocampus in MPS IA participants were smaller than in HC. Age-related curves of the amygdala, thalamus, and globus pallidum volumes diverged from HC but were comparable between MPS I groups. The thalamus serves as a relay point for major WM pathways in the brain⁴³. Thus, a reduced thalamic volume may be secondary to WM pathology (e.g., as found in MS⁴⁴) or primarily due to MPS I GM disease. Primary thalamic pathology seems plausible given the findings in other subcortical GM structures (e.g., globus pallidum and amygdala in MPS IH and MPS IA and hippocampus in

MPS IA). Glycosaminoglycan accumulation was demonstrated in subcortical GM of canine MPS I and cleared after intrathecal ERT⁴⁵. Still, it seems unlikely that GAG clearance explains changes in thalamic or other subcortical volumes as both MPS groups showed similar slopes.

4.5. Ventricles and choroid plexus

Ventriculomegaly is one of the MRI hallmarks in MPS I⁴. Ventricular volume very slowly and steadily increases from infancy through adolescence during normal development⁴⁶. An age-related increase in ventricular and ChP volumes was present in both MPS I groups, whereas in the HC group, no age-related change in these structures was detected. As previously described in MPS I⁵, IQ was negatively associated with ventricular volumes. It is important to note that ventricular and ChP volumes had the highest variability across all measured brain structures, underscoring that MPS I is a phenotypically heterogeneous disease.

The choroid plexus is a structure that produces 70-80% of CSF and regulates the internal CSF microenvironment⁴⁷. During development, the ChP is derived from the intraventricular extension of vascularized leptomeningeal tissue. Therefore, similar GAG storage and size expansion as seen in meninges can be expected in ChP tissue. An autopsy study identified nodular lesions resulting from the proliferation of vacuolated pericytes, fibroblasts, and arachnoid cells in MPS I brains, supporting this hypothesis. These nodular lesions, which may increase the total size of the ChP, were not associated with age, hydrocephalus severity, or enlargement of perivascular spaces in WM⁴⁸. Glycosaminoglycan buildup in the arachnoid granulations has traditionally been believed to be responsible for the decreased CSF clearance into the dural sinuses and the subsequent development of communicating hydrocephalus¹⁶. Choroid plexus hypertrophy leading to excessive CSF production has not been posited as a possible cause of ventriculomegaly in MPS I. Our study revealed a significant correlation between ventricular and ChP volumes (MPS IH > MPS IA > HC), but future studies are necessary to elucidate if a functional relationship exists between ChP enlargement, CSF production, and ventriculomegaly in MPS I.

4.6. Limitations

There are some limitations of this study, particularly the use of cross-sectional data to infer developmental changes. Additionally, true natural history data with “naïve” MPS I participants are unavailable as all patients undergo HSCT or receive intravenous ERT as standard-of-care. Healthy control data acquired on a Philips scanner were not available, though the 3D T1-weighted protocols used on each scanner in this study were uniform. Limited sample size inherent to studying rare diseases reduces the power to identify significant differences and limits the ability to use a more elaborate model to fit developmental curves. Intracranial volume adjustment and its shortcomings, based on estimating ICV^{49, 50} with MRI, has been discussed above (*see* section 4.1.). Finally, participants with ventricular shunts who likely have even more severe brain disease were excluded from the analysis. This is because of the introduction of iatrogenic manipulation of neuroanatomical volume and because susceptibility artifacts incurred by programmable ventriculoperitoneal shunts cause local loss of signal intensity.

5. Conclusion

In this cross-sectional, observational MRI study, quantitatively measured changes in brain macrostructure distinguished participants with MPS I from a cohort of healthy controls and distinguished participants with severe from attenuated forms of MPS I. Morphometric differences in cortical and subcortical gray matter, ventricles, and choroid plexus were documented and quantified in addition to the previously described white matter abnormalities. Further, a longitudinal investigation is needed to confirm the relationships observed in this study and elucidate the impact of this disease on the neurodevelopmental trajectories of individuals with MPS I. Finally, reliable quantitative assessment of MPS brain abnormality is exceedingly desirable for the evaluation of novel CNS-directed treatments.

Acknowledgment

We thank the children and their parents and/or caretakers, and adults with mucopolysaccharidosis for their participation in this study. In addition, we thank Dr. Bruce Fischl from MGH-NMR Center, Harvard University, for his guidance and support in the processing of complicated cases. The authors also thank Brenda Diethelm-Okita, Ashley Schneider (née Wiesenburger), David Erickson, and Evelyn Redtree in the Lysosomal Disease Network office at the University of Minnesota for administrative assistance. Study data were collected and managed with REDCap electronic data capture tools hosted at the University of Minnesota.

The study was funded by the Sanofi Genzyme (GZ-2014-11270), the National MPS Society, Million Dollar Bike Ride from the University of Pennsylvania (MDBR-16-125-MPS, 303052MPSI-16-003-02), the Ryan Foundation, the Rare Diseases Clinical Research Network, Lysosomal Disease Network, NIH U54NS065768, and the resources of the Center for Magnetic Resonance Research (supported by NIBIB P41 EB027061, P30 NS076408, and 1S10OD017974-01), the Center for Neurobehavioral Development, and the Minnesota Supercomputing Institute.

Control data were supported by the NIH (5P41RR008079, 5K12RR023247, P30-NS057091, and MO1-RR00400; K24 MH071434, K24 DA028773, RO1-MH61744, R01-AA12479, and RO1-MH63407 to Master Drug Data Base), Medical Investigation of Neurodevelopmental Disorders Institute, and Gillette Children's Research Fund, Shire/Takeda (4-7-year-old study), and Clinical and Translational Science Institute grant support (UL1TR000114 from the National Center for Advancing Translational Sciences [NCATS] of the NIH). This publication was also supported in part by the NIH NCATS through UCSF-CTSI grant UL1TR000004. Its contents are solely the authors' responsibility and do not necessarily represent the official views of the NIH.

Author disclosures

Victor Kovac reports no disclosures.

Elsa G. Shapiro, Consultant for Shapiro Neuropsychology Consulting LLC

Kyle D. Rudser reports no disclosures.

Bryon Mueller reports no disclosures.

Julie B. Eisengart, Research support from Lysogene, Sangamo, Shire/Takeda and Sobi; consulting fees from ArmaGen, Denali Therapeutics, JCR Pharmaceutical, Orchard Therapeutics, ReGenXBio and Shire/Takeda; and advisory boards for Amicus Therapeutics, bluebird bio, Denali, Orchard Therapeutics, ReGenXBio, Sanofi Genzyme and Shire/Takeda.

Kathleen A. Delaney, employee of BioMarin Pharmaceutical Inc

Alia Ahmed reports no disclosures.

Kelly King, Consultant for Passage Bio, RTI Health Solutions, has received research support from Alexion Pharmaceuticals, Inc, bluebird bio, Magenta Therapeutics, Sanofi Genzyme, Shire/Takeda, and was previously a consultant for Shire Plc, and has done previous contract work for Shapiro Neuropsychology Consulting.

Brianna Yund reports no disclosures.

Morton Cowan, Consultant for SAB, Homology Medicine; DSMB, bluebird, bio; DSMB, Chiesi, Inc; DSMB, Rocket Pharma

Julian Raiman, Travel grants, speaker, consultancy fees, and research grants From Genzyme Sanofi, Takeda/Shire HGT, BioMarin, Actelion, Pfizer, Alexion.

Eva Mamak reports no disclosures.

Paul Harmatz, Consultant for BioMarin, Shire, Genzyme, Chiesi, Inventiva, Paradigm, Ultragenyx, SOBI, JCR, Denali, Orphazyme, RegenXbio, Homology, Audentes, Aeglea, and Sangamo, he has received grants from BioMarin, payments (lectures, speakerships, honoraria) from BioMarin, Chiesi, Ultragenyx, and Orphazyme and travel, accommodations, and/or payments for meeting expenses from BioMarin, Shire, Genzyme, Chiesi, Inventiva, Ultragenyx, SOBI, and RegenXbio.

Suma Shankar reports lecture honoraria from Sanofi Genzyme.

Stephanie Cagle reports no disclosures.

Nadia Ali, Research support from Sanofi Genzyme, Shire Takeda, BioMarin, Amicus, and Pfizer, as well as lecturers' honoraria from Sanofi Genzyme, BioMarin, Amicus, and Vitaflo.

Jeff Wozniak reports no disclosures.

Kelvin Lim reports no disclosures.

Paul Orchard, Consultant for Neurogene, Orchard Therapeutics, Rocket Therapeutics; Clinical Trial Support with Immusoft, Bluebird Bio.

Chester B Whitley, Research support from National Institutes of Health including Lysosomal Disease Network (RDCRN) NIH U54NS065768.

Igor Nestrail, Consultant for ICON, Bioclinica, and Quantims and received research support from Million Dollar Bike Ride - University of Pennsylvania, National MPS Society, Biomarin, Sanofi Genzyme, and Shire/Takeda.

Abbreviations:

qMRI	quantitative magnetic resonance imaging
WM	white matter
GM	gray matter
CTh	cortical thickness
CSA	cortical surface area
ChP	choroid plexus

References

1. Vedolin L, Schwartz IVD, Komlos M, et al. Brain MRI in mucopolysaccharidosis - Effect of aging and correlation with biochemical findings. *Neurology* 2007;69:917–924. [PubMed: 17724296]
2. Wang RY, Cambray-Forker EJ, Ohanian K, et al. Treatment reduces or stabilizes brain imaging abnormalities in patients with MPS I and II. *Mol Genet Metab* 2009;98:406–411. [PubMed: 19748810]
3. Matheus MG, Castillo M, Smith JK, Armao D, Towle D, Muenzer J. Brain MRI findings in patients with mucopolysaccharidosis types I and II and mild clinical presentation. *Neuroradiology* 2004;46:666–672. [PubMed: 15205860]
4. Nestrail I, Vedolin L. Quantitative neuroimaging in mucopolysaccharidoses clinical trials. *Mol Genet Metab* 2017;122S:17–24. [PubMed: 29111092]

5. Shapiro EG, Nestrasil I, Rudser K, et al. Neurocognition across the spectrum of mucopolysaccharidosis type I: Age, severity, and treatment. *Mol Genet Metab* 2015;116:61–68. [PubMed: 26095521]
6. King KE, Rudser KD, Nestrasil I, et al. Attention and corpus callosum volumes in individuals with mucopolysaccharidosis type I. *Neurology* 2019;92:e2321–e2328. [PubMed: 30979856]
7. Chen AH, Harmatz P, Nestrasil I, et al. Intrathecal enzyme replacement for cognitive decline in mucopolysaccharidosis type I, a randomized, open-label, controlled pilot study. *Mol Genet Metab* 2020;129:80–90. [PubMed: 31839529]
8. Nestrasil I, Shapiro E, Svatkova A, et al. Intrathecal enzyme replacement therapy reverses cognitive decline in mucopolysaccharidosis type I. *Am J Med Genet A* 2017;173:780–783. [PubMed: 28211988]
9. Burgaleta M, Johnson W, Waber DP, Colom R, Karama S. Cognitive ability changes and dynamics of cortical thickness development in healthy children and adolescents. *Neuroimage* 2014;84:810–819. [PubMed: 24071525]
10. Lange N, Froimowitz MP, Bigler ED, Lainhart JE, Grp BDC. Associations Between IQ, Total and Regional Brain Volumes, and Demography in a Large Normative Sample of Healthy Children and Adolescents. *Developmental Neuropsychology* 2010;35:296–317. [PubMed: 20446134]
11. Schnack HG, van Haren NEM, Brouwer RM, et al. Changes in Thickness and Surface Area of the Human Cortex and Their Relationship with Intelligence. *Cerebral Cortex* 2015;25:1608–1617. [PubMed: 24408955]
12. Luders E, Narr KL, Thompson PM, Toga AW. Neuroanatomical Correlates of Intelligence. *Intelligence* 2009;37:156–163. [PubMed: 20160919]
13. Fischl B, Salat DH, Busa E, et al. Whole brain segmentation: automated labeling of neuroanatomical structures in the human brain. *Neuron* 2002;33:341–355. [PubMed: 11832223]
14. FreeSurfer: FreeSurfer Release Notes. <https://surfer.nmr.mgh.harvard.edu/fswiki/ReleaseNotes> [computer program] 2017.
15. A language and environment for statistical computing. R Foundation for Statistical Computing, Vienna, Austria. <http://www.R-project.org/> [computer program] 2014.
16. Neufeld E, Muenzer J, Scriver C, Beaudet A, Sly W. *The mucopolysaccharidoses*: McGraw-Hill, 2001.
17. Whitley CB. The mucopolysaccharidoses. In: Beighton P, ed. *McKusick's Heritable Disorders of Connective Tissue*, 5th ed: St Louis, C.V. Mosby, 1993: 367–499.
18. Pastores GM, Arn P, Beck M, et al. The MPS I registry: design, methodology, and early findings of a global disease registry for monitoring patients with Mucopolysaccharidosis Type I. *Mol Genet Metab* 2007;91:37–47. [PubMed: 17336562]
19. Kakkis ED, Muenzer J, Tiller GE, et al. Enzyme-replacement therapy in mucopolysaccharidosis I. *N Engl J Med* 2001;344:182–188. [PubMed: 11172140]
20. Urayama A, Grubb JH, Sly WS, Banks WA. Developmentally regulated mannose 6-phosphate receptor-mediated transport of a lysosomal enzyme across the blood-brain barrier. *Proc Natl Acad Sci U S A* 2004;101:12658–12663. [PubMed: 15314220]
21. Eisengart JB, Rudser KD, Xue Y, et al. Long-term outcomes of systemic therapies for Hurler syndrome: an international multicenter comparison. *Genet Med* 2018;20:1423–1429. [PubMed: 29517765]
22. Vite CH, Nestrasil I, Mlikotic A, et al. Features of brain MRI in dogs with treated and untreated mucopolysaccharidosis type I. *Comp Med* 2013;63:163–173. [PubMed: 23582423]
23. Provenzale JM, Nestrasil I, Chen S, et al. Diffusion tensor imaging and myelin composition analysis reveal abnormal myelination in corpus callosum of canine mucopolysaccharidosis I. *Exp Neurol* 2015;273:1–10. [PubMed: 26222335]
24. Satzer D, DiBartolomeo C, Ritchie MM, et al. Assessment of dysmyelination with RAFFn MRI: application to murine MPS I. *PLoS One* 2015;10:e0116788. [PubMed: 25680196]
25. Le SQ, Nestrasil I, Kan SH, et al. Myelin and Lipid Composition of the Corpus Callosum in Mucopolysaccharidosis Type I Mice. *Lipids* 2020.
26. Loeb H, Jonniaux G, Resibois A, et al. Biochemical and ultrastructural studies in Hurler's syndrome. *J Pediatr* 1968;73:860–874. [PubMed: 4972189]

27. Wilkinson FL, Holley RJ, Langford-Smith KJ, et al. Neuropathology in mouse models of mucopolysaccharidosis type I, IIIA and IIIB. *PLoS One* 2012;7:e35787. [PubMed: 22558223]
28. Shapiro E, Guler OE, Rudser K, et al. An exploratory study of brain function and structure in mucopolysaccharidosis type I: long term observations following hematopoietic cell transplantation (HCT). *Mol Genet Metab* 2012;107:116–121. [PubMed: 22867884]
29. Nestrasil I, Shapiro E, Svatkova A, et al. Intrathecal Enzyme Replacement Therapy Reverses Cognitive Decline in Mucopolysaccharidosis type I. *Am J Med Genet A* 2017;173:780–783. [PubMed: 28211988]
30. Yund B, Rudser K, Ahmed A, et al. Cognitive, medical, and neuroimaging characteristics of attenuated mucopolysaccharidosis type II. *Mol Genet Metab* 2015;114:170–177. [PubMed: 25541100]
31. Tanaka-Arakawa MM, Matsui M, Tanaka C, et al. Developmental changes in the corpus callosum from infancy to early adulthood: a structural magnetic resonance imaging study. *PLoS One* 2015;10:e0118760. [PubMed: 25790124]
32. Bigger BW, Begley DJ, Virgintino D, Pshezhetsky AV. Anatomical changes and pathophysiology of the brain in mucopolysaccharidosis disorders. *Mol Genet Metab* 2018;125:322–331. [PubMed: 30145178]
33. Lee C, Dineen TE, Brack M, Kirsch JE, Runge VM. The mucopolysaccharidoses: characterization by cranial MR imaging. *AJNR Am J Neuroradiol* 1993;14:1285–1292. [PubMed: 8279321]
34. Matheus MG, Castillo M, Smith JK, Armao D, Towle D, Muenzer J. Brain MRI findings in patients with mucopolysaccharidosis types I and II and mild clinical presentation. *Neuroradiology* 2004;46:666–672. [PubMed: 15205860]
35. Labounek R, Mai K, Mueller B, Ellinwood NM, Dickson P, Nestrasil I. In-vivo cortical thickness estimation from high-resolution T1w MRI scans in healthy and mucopolysaccharidosis affected dogs. *Conf Proc IEEE Eng Med Biol Soc* 2019;2019:2848–2851.
36. Lemaitre H, Goldman AL, Sambataro F, et al. Normal age-related brain morphometric changes: nonuniformity across cortical thickness, surface area and gray matter volume? *Neurobiol Aging* 2012;33:617 e611–619.
37. Burgaleta M, Johnson W, Waber DP, Colom R, Karama S. Cognitive ability changes and dynamics of cortical thickness development in healthy children and adolescents. *Neuroimage* 2014;84:810–819. [PubMed: 24071525]
38. Ou L, Herzog T, Koniar BL, Gunther R, Whitley CB. High-dose enzyme replacement therapy in murine Hurler syndrome. *Mol Genet Metab* 2014;111:116–122. [PubMed: 24100243]
39. Dickson P, McEntee M, Vogler C, et al. Intrathecal enzyme replacement therapy: successful treatment of brain disease via the cerebrospinal fluid. *Mol Genet Metab* 2007;91:61–68. [PubMed: 17321776]
40. Giedd JN, Rapoport JL. Structural MRI of pediatric brain development: what have we learned and where are we going? *Neuron* 2010;67:728–734. [PubMed: 20826305]
41. Aleman-Gomez Y, Janssen J, Schnack H, et al. The human cerebral cortex flattens during adolescence. *J Neurosci* 2013;33:15004–15010. [PubMed: 24048830]
42. Narvacan K, Treit S, Camicioli R, Martin W, Beaulieu C. Evolution of deep gray matter volume across the human lifespan. *Hum Brain Mapp* 2017;38:3771–3790. [PubMed: 28548250]
43. Haber SN, Calzavara R. The cortico-basal ganglia integrative network: the role of the thalamus. *Brain Res Bull* 2009;78:69–74. [PubMed: 18950692]
44. Azevedo CJ, Cen SY, Khadka S, et al. Thalamic atrophy in multiple sclerosis: A magnetic resonance imaging marker of neurodegeneration throughout disease. *Ann Neurol* 2018;83:223–234. [PubMed: 29328531]
45. Chen A, Vogler C, McEntee M, et al. Glycosaminoglycan storage in neuroanatomical regions of mucopolysaccharidosis I dogs following intrathecal recombinant human iduronidase. *APMIS* 2011;119:513–521. [PubMed: 21749451]
46. McAllister A, Leach J, West H, Jones B, Zhang B, Serai S. Quantitative Synthetic MRI in Children: Normative Intracranial Tissue Segmentation Values during Development. *AJNR Am J Neuroradiol* 2017;38:2364–2372. [PubMed: 28982788]

47. Liddelow SA. Development of the choroid plexus and blood-CSF barrier. *Front Neurosci* 2015;9:32. [PubMed: 25784848]
48. Lach B, Haust MD. Nodular lesions of choroid plexus in Hurler disease. *Fetal Pediatr Pathol* 2011;30:189–198. [PubMed: 21355678]
49. Heinen R, Bouvy WH, Mendrik AM, Viergever MA, Biessels GJ, de Bresser J. Robustness of Automated Methods for Brain Volume Measurements across Different MRI Field Strengths. *PLoS One* 2016;11:e0165719. [PubMed: 27798694]
50. Malone IB, Leung KK, Clegg S, et al. Accurate automatic estimation of total intracranial volume: a nuisance variable with less nuisance. *Neuroimage* 2015;104:366–372. [PubMed: 25255942]

Highlights

- Quantitatively measured brain macrostructure distinguished MPS I and healthy subjects
- Brain MRI volumes differed in participants with severe and attenuated MPS I forms
- In addition to white matter, other brain regions showed morphometric changes
- Cortical and subcortical gray matter, ventricles, and choroid plexus were altered
- IQ-related associations to ventricular volume and cortical thickness were present

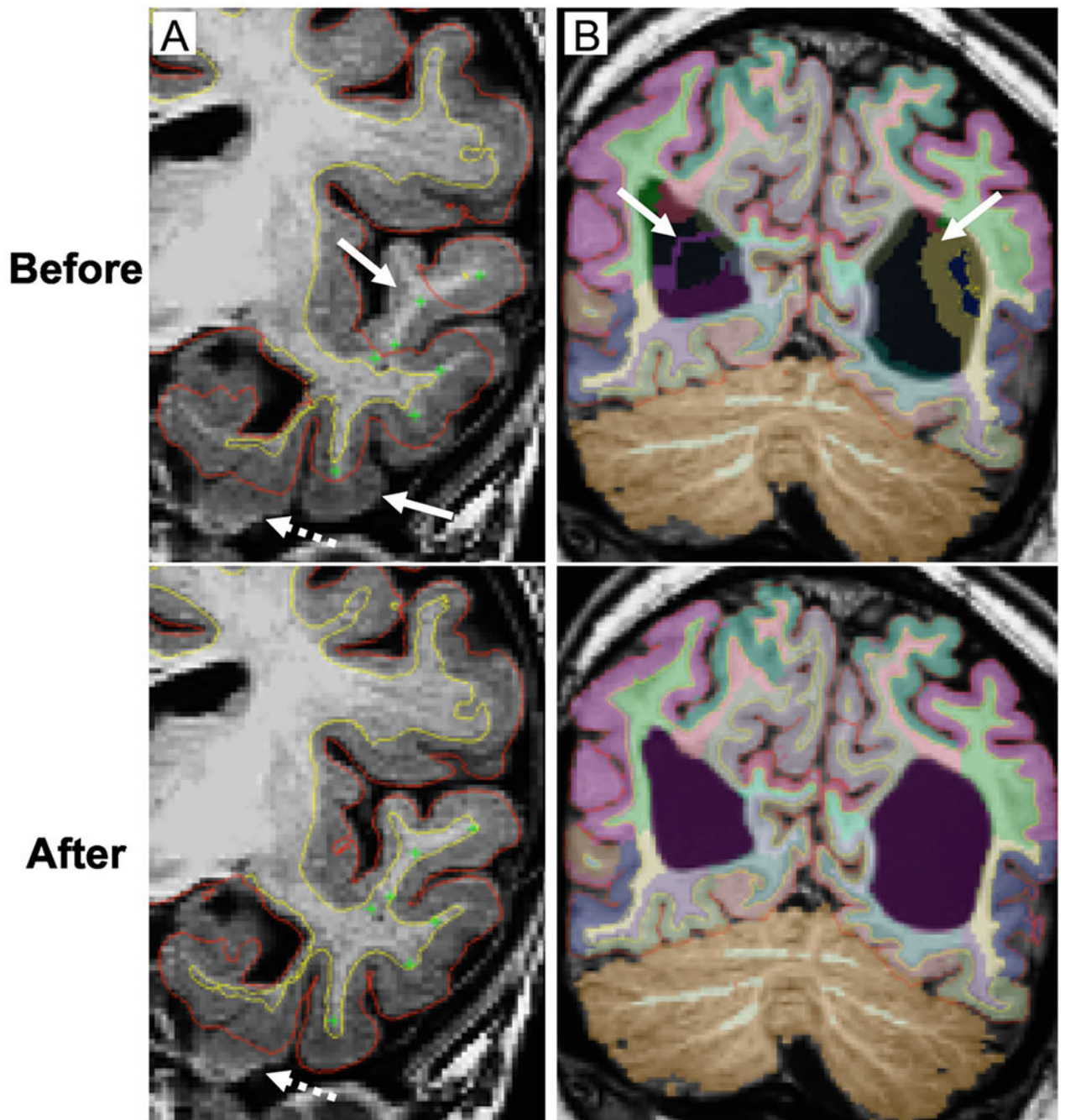


Figure 1.

Corrections of automated brain MRI segmentation in MPS I participants.

Coronal T1-weighted images. Pial surface – red line, cerebral white matter surface – yellow line. **A.** White and gray matter segmentation of the left temporal lobe with the placement of control points (green cross) in the under-segmented white matter (arrows).

Edited scans before and after an iteration of automated segmentation. Relatively small parts of mesiotemporal structures may remain unsegmented (dashed arrow) due to the low gray/white matter contrast.

B. Brain mislabeling at the level of lateral ventricles (purple label)

due to the prominent ventricular enlargement (arrows). Scans are shown before and after an iteration of automated segmentation with *-bigventricles* flag. Color-coded labels overlaid on T1-weighted image correspond to specific brain regions.

Author Manuscript

Author Manuscript

Author Manuscript

Author Manuscript

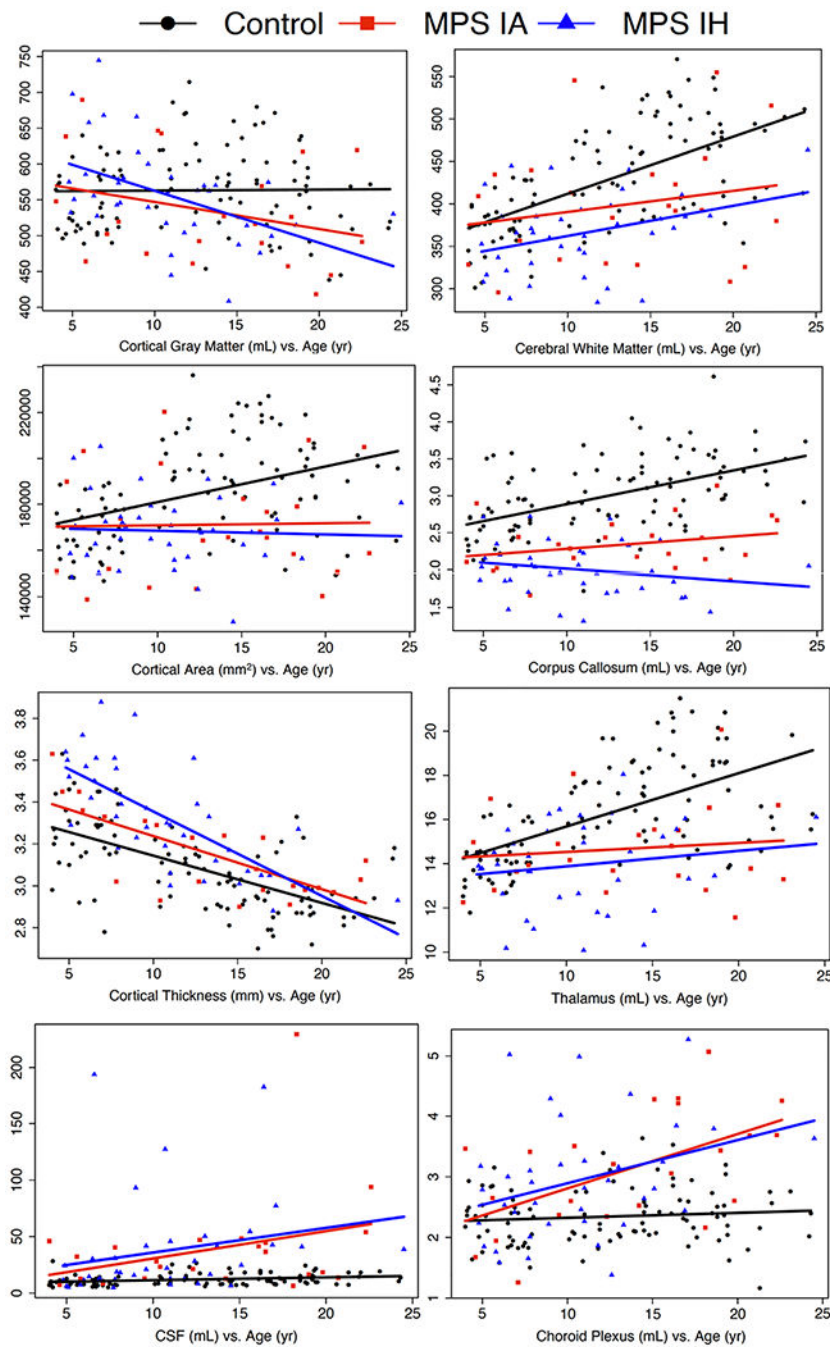


Figure 2. Brain MRI measure vs. age for MPS IA and MPS IH participants and healthy controls. Age in years on the x-axis, brain MRI measure on the y-axis. **HC** healthy control, **MPS IA** attenuated form of mucopolysaccharidosis type I, **MPS IH** severe form of mucopolysaccharidosis type I, **CSF** cerebrospinal fluid, corresponds to total ventricular volume.

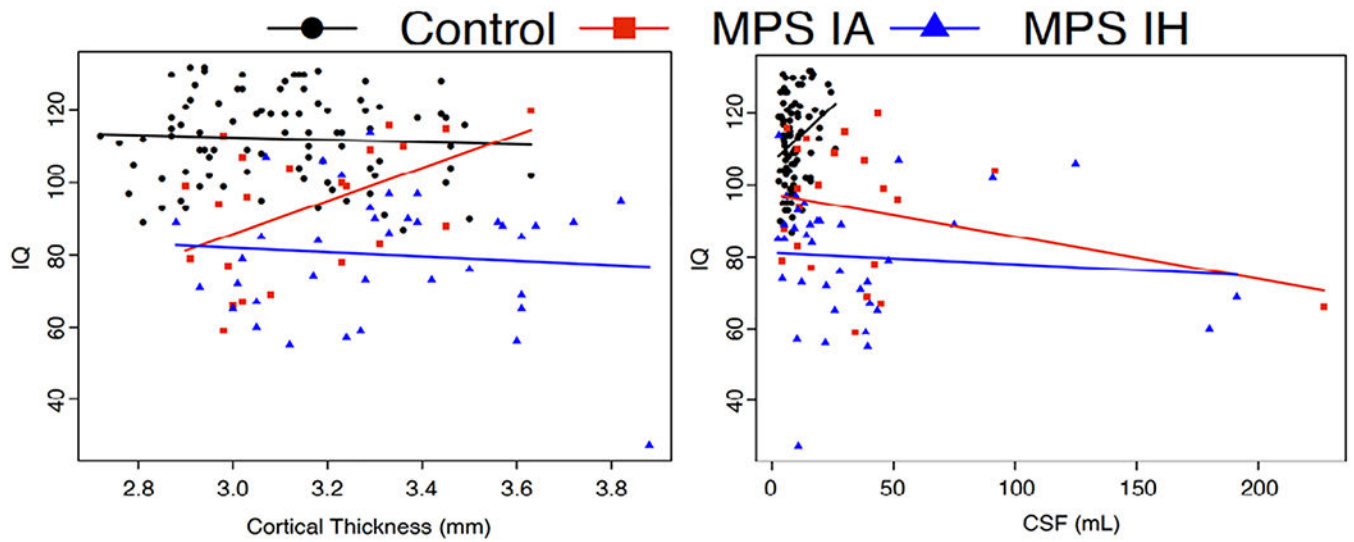


Figure 3.

Cortical thickness and ventricular volume (CSF) vs. IQ for MPS IA and MPS IH participants and healthy controls.

Brain measure on the x-axis, IQ score on the y-axis. **HC** healthy control, **MPS IA** attenuated form of mucopolysaccharidosis type I, **MPS IH** severe form of mucopolysaccharidosis type I, **CSF** cerebrospinal fluid, corresponds to total ventricular volume.

Table 1

Demographic characteristics.

Covariate	HC (N=98)	MPS IA (N=23)	MPS IH (N=38)
Female	54 (55.1%)	12 (52.2%)	21 (55.3%)
Site			
UMN	98 (100.0%)	18 (78.3%)	31 (81.6%)
EU	0 (0.0%)	1 (4.3%)	0 (0.0%)
OC	0 (0.0%)	1 (4.3%)	0 (0.0%)
SF	0 (0.0%)	0 (0.0%)	4 (10.5%)
SK	0 (0.0%)	3 (13.0%)	3 (7.9%)
Age (years)	12.5 (5.7)	13.4 (5.9)	10.6 (4.5)
Age at diagnosis (years)	n/a	5.2 (3.3)	1.0 (0.7)
Missing age at dx	n/a	3 (13.0%)	1 (2.63%)
IQ	112 (12.0)	93.1 (18.4)	80.0 (17.6)
Missing IQ	9 (9.18%)	1 (4.35%)	1 (2.63%)

Values presented are mean (standard deviation) or N (%) where indicated.

MPS IA attenuated form of mucopolysaccharidosis type I, **MPS IH** severe form of mucopolysaccharidosis type I, **HC** healthy controls, **UMN** University of Minnesota; **EU** Emory University; **OC** Oakland; **SF** San Francisco, **SK** SickKids Toronto;

n/a not available.

Table 2

Brain MRI measures characteristics.

Covariate	HC	MPS IA	MPS IH	P-value	P-value
	(N=98)	(N=23)	(N=38)	IA vs. HC	IH vs. HC
Cortical GM (mL)	563 (58.2)	534 (74.9)	558 (67.3)	0.059	0.491
Cortical SA (mm ²)	184830 (21313.9)	171177 (23731.3)	168401 (15814.5)	0.002	<0.001
CTh (mm)	3.1 (0.2)	3.1 (0.2)	3.3 (0.3)	<i>0.025</i>	<0.001
Cerebral WM (mL)	429 (62.7)	399 (71.8)	364 (46.7)	0.005	<0.001
CC (mL)	3.0 (0.5)	2.3 (0.4)	2.0 (0.4)	<0.001	<0.001
Cerebellar WM (mL)	29.0 (4.4)	30.3 (6.5)	29.5 (5.9)	0.397	0.144
Cerebellar GM (mL)	114 (11.9)	112 (11.4)	107 (14.9)	0.399	<i>0.015</i>
Ventricles (mL)	12.0 (5.2)	38.9 (46.3)	37.2 (44.2)	<0.001	<0.001
Choroid plexus (mL)	2.3 (0.5)	3.1 (1.0)	2.9 (1.0)	<0.001	<0.001
Thalamus (mL)	16.3 (2.3)	14.7 (2.0)	13.9 (2.0)	<0.001	<0.001
Hippocampus (mL)	8.5 (0.9)	8.1 (0.9)	8.3 (0.9)	<i>0.037</i>	0.351
Amygdala (mL)	3.2 (0.5)	3.1 (0.4)	3.1 (0.4)	0.073	0.474
Pallidum (mL)	3.7 (0.5)	3.4 (0.4)	3.3 (0.7)	0.01	<0.001
Putamen (mL)	12.3 (1.6)	12.2 (1.0)	11.7 (1.6)	0.636	0.054
Caudate (mL)	8.4 (1.2)	8.4 (1.5)	8.3 (1.4)	0.877	0.878
ICV (mL)	1592 (196.7)	1628 (277.0)	1547 (249.8)	0.667	0.648

Values presented are mean (standard deviation).

P-values for differences in means for each of MPS IA and MPS IH vs. healthy HC.

MPS IA attenuated form of mucopolysaccharidosis type I, **MPS IH** severe form of mucopolysaccharidosis type I, **HC** healthy controls, **GM** gray matter, **SA** surface area, **CTh** mean cortical thickness, **WM** white matter, **CC** corpus callosum, **ICV** intracranial volume. **P-values** 0.05 in italic, 0.01 in bold.

Table 3

Brain MRI measures and age.

A. Age-related differences in brain MRI measures for MPS IA, MPS IH participants, and HC.

Volume (mL)/thickness (mm)/area (mm ²)	Group Age (per year)	Mean Difference (95% CI)	P-value	ICV adjusted vol; P-value
Amygdala	MPS IA	0.00 (-0.03, 0.02)	0.743	0.167
	MPS IH	-0.01 (-0.03, 0.02)	0.672	0.102
	HC	0.04 (0.03, 0.06)	<0.001	0.201
Caudate	MPS IA	0.04 (-0.05, 0.14)	0.379	0.645
	MPS IH	0.01 (-0.08, 0.10)	0.853	0.096
	HC	0.07 (0.03, 0.11)	<0.001	0.358
Corpus callosum	MPS IA	0.02 (-0.01, 0.04)	0.209	0.979
	MPS IH	-0.02 (-0.04, 0.01)	0.160	0.011
	HC	0.05 (0.03, 0.06)	<0.001	0.044
Cerebellar GM	MPS IA	0.30 (-0.42, 1.02)	0.413	0.325
	MPS IH	0.18 (-0.65, 1.00)	0.672	0.074
	HC	0.62 (0.23, 1.00)	0.002	0.003
Cerebellar WM	MPS IA	0.39 (-0.01, 0.79)	0.054	0.214
	MPS IH	0.22 (-0.10, 0.54)	0.181	0.956
	HC	0.45 (0.33, 0.58)	<0.001	0.010
Cerebral WM	MPS IA	2.49 (-2.50, 7.49)	0.328	0.954
	MPS IH	3.55 (0.55, 6.55)	0.020	0.504
	HC	6.74 (5.03, 8.44)	<0.001	<0.001
Choroid plexus	MPS IA	0.09 (0.03, 0.14)	0.001	0.012
	MPS IH	0.07 (0.02, 0.13)	0.012	0.045
	HC	0.01 (-0.01, 0.02)	0.305	0.019
Cortical Surface Area	MPS IA	89.70 (-1658.82, 1838.23)	0.920	0.080
	MPS IH	-162.01 (-1313.39, 989.37)	0.783	0.003
	HC	1556.52 (900.29, 2212.74)	<0.001	0.126
Cortical GM	MPS IA	-3.77 (-9.28, 1.75)	0.181	<0.001
	MPS IH	-7.25 (-11.65, -2.86)	0.001	<0.001
	HC	0.13 (-1.74, 2.01)	0.889	<0.001
Hippocampus	MPS IA	0.01 (-0.05, 0.06)	0.783	0.298
	MPS IH	-0.01 (-0.08, 0.06)	0.755	0.080
	HC	0.05 (0.02, 0.08)	<0.001	0.004
Mean Cortical Thickness	MPS IA	-0.03 (-0.04, -0.02)	<0.001	0.016
	MPS IH	-0.04 (-0.05, -0.03)	<0.001	<0.001
	HC	-0.02 (-0.03, -0.02)	<0.001	<0.001
Pallidum	MPS IA	-0.03 (-0.06, 0.01)	0.102	0.003
	MPS IH	0.02 (-0.02, 0.06)	0.268	0.864
	HC	0.02 (0.00, 0.04)	0.069	<0.001
Putamen	MPS IA	-0.01 (-0.08, 0.06)	0.727	0.193
	MPS IH	-0.04 (-0.13, 0.06)	0.457	0.008

A. Age-related differences in brain MRI measures for MPS IA, MPS IH participants, and HC.

Volume (mL)/thickness (mm)/area (mm ²)	Group Age (per year)	Mean Difference (95% CI)	P-value	ICV adjusted vol; P-value
Thalamus	HC	0.07 (0.02, 0.12)	0.005	0.008
	MPS IA	0.04 (-0.10, 0.19)	0.580	0.339
	MPS IH	0.07 (-0.03, 0.17)	0.188	0.425
Ventricles	HC	0.24 (0.17, 0.31)	<0.001	<0.001
	MPS IA	2.42 (-0.42, 5.26)	0.094	0.117
	MPS IH	2.19 (-0.86, 5.23)	0.159	0.095
	HC	0.25 (0.09, 0.42)	0.002	0.096

B. Comparison of linear trends between MPS IA, MPS IH participants, and HC vs. age.

Volume (mL)/thickness (mm)/area (mm ²)	Group comparison (per year of age)	Mean Difference (95% CI)	P-value	ICV-adjusted vol; P-value
Amygdala	MPS IA vs. HC	0.05 (0.01, 0.08)	0.005	0.078
	MPS IA vs. MPS IH	0.00 (-0.04, 0.04)	0.956	0.956
	HC vs. MPS IH	0.05 (0.02, 0.08)	0.003	0.044
Caudate	MPS IA vs. HC	0.03 (-0.08, 0.13)	0.616	0.951
	MPS IA vs. MPS IH	-0.03 (-0.17, 0.10)	0.614	0.431
	HC vs. MPS IH	0.06 (-0.04, 0.16)	0.238	0.359
Corpus callosum	MPS IA vs. HC	0.03 (0.00, 0.06)	0.056	0.321
	MPS IA vs. MPS IH	-0.03 (-0.07, 0.00)	0.062	0.110
	HC vs. MPS IH	0.06 (0.04, 0.09)	<0.001	0.001
Cerebellar GM	MPS IA vs. HC	0.32 (-0.50, 1.13)	0.449	0.884
	MPS IA vs. MPS IH	-0.12 (-1.21, 0.97)	0.826	0.790
	HC vs. MPS IH	0.44 (-0.47, 1.35)	0.346	0.835
Cerebellar WM	MPS IA vs. HC	0.06 (-0.36, 0.48)	0.775	0.929
	MPS IA vs. MPS IH	-0.17 (-0.69, 0.34)	0.503	0.312
	HC vs. MPS IH	0.24 (-0.11, 0.58)	0.178	0.187
Cerebral WM	MPS IA vs. HC	4.25 (-1.03, 9.52)	0.115	0.054
	MPS IA vs. MPS IH	1.06 (-4.77, 6.88)	0.722	0.619
	HC vs. MPS IH	3.19 (-0.26, 6.64)	0.070	0.172
Choroid plexus	MPS IA vs. HC	-0.08 (-0.14, -0.02)	0.005	0.002
	MPS IA vs. MPS IH	-0.02 (-0.10, 0.06)	0.641	0.727
	HC vs. MPS IH	-0.06 (-0.12, -0.01)	0.032	0.011
Cortical Surface Area	MPS IA vs. HC	1466.81 (-400.80, 3334.42)	0.124	0.386
	MPS IA vs. MPS IH	-251.71 (-2345.28, 1841.85)	0.814	0.452
	HC vs. MPS IH	1718.53 (393.27, 3043.79)	0.011	0.062
Cortical GM	MPS IA vs. HC	3.90 (-1.92, 9.72)	0.189	0.492
	MPS IA vs. MPS IH	-3.49 (-10.54, 3.57)	0.332	0.070
	HC vs. MPS IH	7.39 (2.61, 12.17)	0.002	0.004
Hippocampus	MPS IA vs. HC	0.04 (-0.02, 0.10)	0.195	0.962
	MPS IA vs. MPS IH	-0.02 (-0.11, 0.07)	0.678	0.566
	HC vs. MPS IH	0.06 (-0.01, 0.13)	0.104	0.429

A. Age-related differences in brain MRI measures for MPS IA, MPS IH participants, and HC.

Volume (mL)/thickness (mm)/area (mm ²)	Group Age (per year)	Mean Difference (95% CI)	P-value	ICV adjusted vol; P-value
Mean Cortical Thickness	MPS IA vs. HC	0.00 (-0.01, 0.01)	0.637	0.597
	MPS IA vs. MPS IH	-0.01 (-0.03, 0.00)	0.056	0.431
	HC vs. MPS IH	0.02 (0.00, 0.03)	0.009	0.626
Pallidum	MPS IA vs. HC	0.04 (0.01, 0.08)	<i>0.019</i>	0.125
	MPS IA vs. MPS IH	0.05 (0.00, 0.09)	0.057	0.060
	HC vs. MPS IH	0.00 (-0.04, 0.04)	0.880	0.323
Putamen	MPS IA vs. HC	0.08 (0.00, 0.16)	0.053	0.702
	MPS IA vs. MPS IH	-0.02 (-0.14, 0.09)	0.680	0.603
	HC vs. MPS IH	0.11 (0.00, 0.22)	0.054	0.194
Thalamus	MPS IA vs. HC	0.20 (0.04, 0.36)	<i>0.015</i>	<i>0.036</i>
	MPS IA vs. MPS IH	0.03 (-0.15, 0.21)	0.748	0.873
	HC vs. MPS IH	0.17 (0.05, 0.30)	0.008	<i>0.043</i>
Ventricles	MPS IA vs. HC	-2.17 (-5.01, 0.67)	0.135	0.148
	MPS IA vs. MPS IH	-0.24 (-4.40, 3.93)	0.911	0.803
	HC vs. MPS IH	-1.93 (-4.98, 1.12)	0.214	0.117

Differences showed per year of age.

MPS IA attenuated form of mucopolysaccharidosis type I, **MPS IH** severe form of mucopolysaccharidosis type I, **HC** healthy controls, **GM** gray matter, **WM** white matter, **ICV** intracranial volume. **CI** confidence interval. P-values are presented for ICV non-adjusted volumes (**P-value**) and ICV-adjusted brain volumes (**ICV adjusted Vol; P-value**). **P-values** 0.05 in italic, 0.01 in bold.

Table 4

Brain MRI measures and IQ.

A. Brain MRI measure vs. IQ for MPS IA, MPS IH participants, and HC				
Predictor	Group	IQ mean difference (95% CI)	P-value	ICV-adjusted vol; P-value
Cortical thickness (per mm)	MPS IA	45.77 (16.65, 74.89)	0.002	0.355
	MPS IH	-5.94 (-34.28, 22.41)	0.681	0.753
	HC	-3.28 (-15.56, 9.00)	0.601	<0.001
Cortical GM (per mL)	MPS IA	0.09 (0.02, 0.16)	0.008	0.056
	MPS IH	0.02 (-0.09, 0.12)	0.765	0.770
	HC	0.09 (0.06, 0.12)	<0.001	0.797
Cortical SA (per mm ²)	MPS IA	0.12 (-0.17, 0.41)	0.430	0.447
	MPS IH	0.19 (-0.11, 0.49)	0.209	0.429
	HC	0.20 (0.10, 0.31)	<0.001	0.276
Cerebral WM (per mL)	MPS IA	0.00 (-0.10, 0.11)	0.929	0.934
	MPS IH	0.03 (-0.09, 0.14)	0.641	0.358
	HC	0.07 (0.03, 0.11)	<0.001	0.871
Thalamus (per mL)	MPS IA	1.01 (-2.82, 4.84)	0.604	0.608
	MPS IH	1.66 (-0.26, 3.58)	0.090	0.150
	HC	2.00 (1.04, 2.96)	<0.001	0.728
Ventricles (per mL)	MPS IA	-0.12 (-0.19, -0.04)	0.002	<i>0.014</i>
	MPS IH	-0.03 (-0.15, 0.09)	0.599	0.549
	HC	0.62 (0.20, 1.05)	0.004	0.122
B. Comparison of linear trends between MPS IA, MPS IH participants, and HC vs. IQ				
Predictor	Group	IQ slope difference (95% CI)	P-value	ICV-adjusted vol; P-value
Cortical thickness (per mm)	MPS IA vs. HC	-49.05 (-80.65, -17.45)	0.002	<i>0.029</i>
	MPS IA vs. MPS IH	-51.71 (-92.34, -11.07)	<i>0.013</i>	0.352
	HC vs. MPS IH	2.66 (-28.23, 33.54)	0.866	0.153
Cortical GM (per mL)	MPS IA vs. HC	0.00 (-0.07, 0.07)	0.969	0.068
	MPS IA vs. MPS IH	-0.07 (-0.20, 0.05)	0.242	0.224
	HC vs. MPS IH	0.07 (-0.04, 0.18)	0.194	0.704
Cortical SA (per mm ²)	MPS IA vs. HC	0.09 (-0.22, 0.40)	0.580	0.266
	MPS IA vs. MPS IH	0.08 (-0.34, 0.49)	0.723	0.981
	HC vs. MPS IH	0.01 (-0.31, 0.33)	0.942	0.245
Cerebral WM (per mL)	MPS IA vs. HC	0.06 (-0.05, 0.17)	0.258	0.882
	MPS IA vs. MPS IH	0.02 (-0.13, 0.18)	0.776	0.560
	HC vs. MPS IH	0.04 (-0.08, 0.16)	0.497	0.532
Thalamus (per mL)	MPS IA vs. HC	0.99 (-2.96, 4.93)	0.624	0.788
	MPS IA vs. MPS IH	0.65 (-3.63, 4.93)	0.767	0.792
	HC vs. MPS IH	0.34 (-1.81, 2.48)	0.757	0.449
Ventricles (per mL)	MPS IA vs. HC	0.74 (0.31, 1.17)	<0.001	<i>0.034</i>
	MPS IA vs. MPS IH	0.09 (-0.06, 0.23)	0.234	0.291

A. Brain MRI measure vs. IQ for MPS IA, MPS IH participants, and HC

Predictor	Group	IQ mean difference (95% CI)	P-value	ICV-adjusted vol; P-value
	HC vs. MPS IH	0.66 (0.22, 1.10)	<i>0.003</i>	0.098

MPS IA attenuated form of mucopolysaccharidosis type I, MPS IH severe form of mucopolysaccharidosis type I, HC healthy controls, GM gray matter, SA surface area, WM white matter, ICV intracranial volume, CI confidence interval. P-values are presented for ICV non-adjusted volumes (P-value) and ICV-adjusted brain volumes (ICV-adjusted vol; P-value). P-values 0.05 in italic, 0.01 in bold.

Author Manuscript

Author Manuscript

Author Manuscript

Author Manuscript